CHEMOTACTIC CELL AGGREGATION VIEWED AS INSTABILITY AND PHASE SEPARATION

KYUNGHAN CHOI AND YONG-JUNG KIM

Abstract. The dynamics in the pattern formation of a chemotaxis cell aggregation model is studied when density-suppressed motility is used. We present four types of cell aggregation patterns depending on the parameter regimes and the mean population density, which are peaks, hot spots, cold spots, and stripes. The analysis is done in two ways. First, the classical instability analysis is used to find two critical densities, where cell aggregation starts when the mean population is between the two values. Second, the phase separation method using van der Waals' double well potential is used to find a population range of pattern formation that is greater than the one the instability analysis gives.

1. Introduction

The purpose of the paper is to classify four types of cell aggregation patterns in a chemotaxis model,

$$\begin{cases} u_t = \Delta(\gamma(v)u^m), & x \in \Omega, t > 0, \\ v_t = \varepsilon\Delta v + u - v, & x \in \Omega, t > 0, \\ \partial_\nu u = \partial_\nu v = 0, & x \in \partial\Omega, t > 0, \\ u(x,0), v(x,0) > 0, & x \in \Omega, \end{cases} \tag{1.1}$$

and introduce the phase separation theory to cell aggregation problems to identify the structure of the aggregation pattern. The motility function of the model is given by

$$\gamma(v) = a + \frac{b}{(d+v)^c} \quad \text{for} \quad b, c > 0, \text{ and } a, d \geq 0. \tag{1.2}$$

The domain $\Omega \subset \mathbb{R}^n$ is bounded with a smooth boundary, and the initial values are bounded. In chemotaxis theory, the unknown solution u is the cell (or amoeba) density, and v is the chemical (or acrasin) density produced by the cells. Nonlinear diffusion is taken with $m > 0$, which is believed to fit as the diffusion of biological organisms. This chemotactic cell aggregation model provides various patterns, such as classical single-point concentrating peaks, uniformly bounded cold and hot spots, and stripe patterns. Peak solutions are known well in chemotaxis theory (see [17, 19, 20]) These four types of patterns fill the missing patterns of chemotaxis theory which are observed in many other fields. We will see that this model connects the chemotaxis theory to the phase separation one.

The chemotaxis model (1.1) can be considered a special case of the Keller-Segel equation, but is based on the opposite concept. The Keller-Segel equation for cell

aggregation phenomena is written as

$$u_t = \nabla \cdot \big(\mu(v)\big(\nabla u - \chi(v)\frac{u}{v}\nabla v\big)\big), \tag{1.3}$$

$$v_t = \varepsilon\Delta v + u - v, \tag{1.4}$$

where $\mu(v)$ the diffusivity of cells, and $\chi(v)$ the chemosensitivity (see [15, (3)–(5)]). The equation (1.3) contains a Fickian diffusion $\mu(v)\nabla u$ and a logarithmic chemotactic advection $-\mu(v)\chi(v)\frac{u}{v}\nabla v$. The fundamental hypothesis on which the model is based is that microorganisms actively sense the macroscopic-scale chemical gradient ∇v to find the direction toward the source, but chemotaxis disappears in the absence of sensing the gradient. Keller and Segel said in their seminal paper [14] that "even though a cell may not be capable of making an accurate assessment of the gradient to which it is exposed at a given time, its average behavior can nevertheless reflect the gradient with arbitrary accuracy." Under the hypothesis, there have been many studies to model the gradient sensing mechanism, and $\mu(v)$ and $\chi(v)$ are taken independently under such a hypothesis. In particular, Keller and Segel assumed that amoebae are sensitive to the relative chemical gradient and hence took the logarithmic model [14, (2.3)].

The model (1.1) is based on the theory that the random dispersal is not given as Fick's diffusion, but as a Fokker-Plank type diffusion,

$$u_t = \Delta(\gamma(v)u), \tag{1.5}$$

where the motility $\gamma(v)$ is the migration rate (see Appendix A). We may write it in the form of a logarithmic chemotaxis model as

$$u_t = \nabla \cdot \Big(\gamma(v)\big(\nabla u - \chi(v)\frac{u}{v}\nabla v\big)\Big),$$

where the chemosensitivity $\chi(v)$ is given by a relation

$$\chi(v) = -\frac{v\gamma'(v)}{\gamma(v)}. \tag{1.6}$$

In other words, the random diffusion model (1.5) is a special case of the chemotaxis model (1.3) when the diffusivity and the chemosensitivity satisfy the relation (1.6) but are not given independently. It is just the randomness, not efforts of microorganisms to sense the chemical gradient, that gives chemotaxis in the model (1.1). Yoon and Kim introduced a consumption model using the random diffusion in [24] and then an aggregation model in [25]. See [3, 4, 6, 9] for the derivation of a related diffusion model.

There are two requirements to be a meaningful chemotaxis model. First, a chemotaxis model should provide appropriate cell aggregation patterns. Keller and Segel [14] viewed the initiation of cell aggregation as instability of constant steady states, which we will follow. However, we will go one step further and investigate the cell aggregation pattern in (1.1) using a phase separation theory. This technique gives information about the structure of the pattern as well as the generation of it. The second requirement is the solution existence. The global well-posedness of Keller-Segel equations has taken a lot of attention. However, the global existence of the logarithmic model has not been obtained in a parameter regime where patterns occur. Recently, the global existence of various chemotaxis models taking (1.5) together with (1.4) or their variations is actively studied (see [7, 8, 11, 23]). These studies indicate that the relation (1.6) helps to obtain the global existence of the

solution of such logarithmic chemotaxis models. These models are also studied with a population growth term in [10, 13].

The diffusion in (1.5) has been generalized in (1.1) by taking an exponent $m > 0$. Under this generalization, the first equation of (1.1) is written as

$$u_t = \nabla \cdot \Big(m\gamma(v) u^{m-1} \Big(\nabla u - \chi(v) \frac{u}{v} \nabla v \Big) \Big),$$

and the corresponding chemosensitivity $\chi(v)$ is

$$\chi(v) := -\frac{v\gamma'(v)}{m\gamma(v)}.$$

We call $v > 0$ an excitable density if $\chi(v) > 1$ and denote the collection of all excitable density values by E, i.e.,

$$E := \{ v \in \mathbb{R}^+ | \chi(v) > 1 \}.$$

Let μ_1 be the principal eigenvalue of the operator $-\Delta$ on Ω under the Neumann boundary condition and denote

$$\varepsilon_1 := -\frac{1}{\mu_1} \Big(1 + \frac{\bar{v}\gamma'(\bar{v})}{m\gamma(\bar{v})} \Big) = -\frac{1}{\mu_1} (1 - \chi(\bar{v}))$$

for a constant $\bar{v} > 0$. We show in Theorem 3.2 that a constant steady state solution $(\bar{u}, \bar{v})$ is linearly unstable if $\varepsilon_1 > 0$ and $0 < \varepsilon < \varepsilon_1$. Therefore, if $\bar{v} \in E$, $\varepsilon_1 > 0$ and an aggregation will occur when $\varepsilon < \varepsilon_1$. If γ is given by (1.2), $a = 0$, and $c > m$, then the excitable density set E is unbounded, and cells aggregate into peaks (see Theorem 3.3). If $a > 0$, $c > m$, and d is small, the excitable density set E is a bounded interval, and cells aggregate into three different patterns of hot spots, cold spots, and stripes depending on the population size.

Note that the instability of a constant steady state $(\bar{u}, \bar{v})$ provides the emergence of an aggregation pattern, but not its shape. Furthermore, the stability is only under a small perturbation. Even if $\bar{v} \notin E$, a pattern may develop under a large perturbation. We take the phase separation theory of Carr, Gurtin, and Slemrod [2] to find further stable nonconstant solutions and their structure (see also [18]). For the case with $a > 0$, we employ a Van der Waals double-well potential given by

$$W(v) = \int_0^v f(s) ds, \quad f(v) := v - K_0 \frac{(d+v)^{c/m}}{(a(d+v)^c + b)^{1/m}},$$

where K_0 is the unique constant that makes $f(v)$ a balanced bi-stable nonlinearity, i.e., there exist three positive zeros of $f(v)$, $\alpha < \mu < \beta$, such that $\int_\alpha^\beta f(s) ds = 0$. Such a coefficient K_0 exists if and only if $E \neq \emptyset$. If $\bar{v} \in (\alpha, \beta)$ and $\varepsilon > 0$ is small enough, there exists a function $v \in H^1(\Omega)$ that minimizes the energy defined by

$$\int_\Omega \big(W(v(x)) + \frac{1}{2} \varepsilon v'(x)^2 \big) dx. \tag{1.7}$$

In the one space dimension with $\Omega = (0, \ell)$, the minimum energy solution is monotone and is the monotone solution of the elliptic problem of (1.1). A constant state $\bar{v} \in (\alpha, \beta)$ is called a separable phase and $E \subset (\alpha, \beta)$. If $\bar{v} \notin (\alpha, \beta)$, the constant steady state $(\bar{u}, \bar{v})$ is stable even under a large perturbation.

The paper is organized as follows. In Section 2, we derive our model system (1.1)–(1.2) from a mesoscopic-scale model with constant diffusivities. We will see that the random diffusion (1.5) naturally appears, and it is more natural for the motility function γ in (1.2) having $a \neq 0$. A bifurcation phenomenon of the model

is discussed. In Section 3, linear stability analysis for constant steady states of (1.1) are given. The excitable density set E is characterized when the motility function is given by (1.2). In Section 4, four kinds of cell aggregation patterns are observed numerically. If $\bar{v} \in E$, a pattern appears for any perturbation, if $\bar{v} \in (\alpha, \beta) \setminus E$, a pattern appears for a large perturbation size, and if $\bar{v} \notin (\alpha, \beta)$, any pattern never appears. In Section 5, we consider the elliptic problem for the steady state of (1.1) in the one space dimension and then transform it into a minimization problem with the energy function in (1.7). The phase separation theory is applied to obtain the minimum energy solution of the elliptic problem and its structure. The conclusions and discussions are given in Section 6.

2. Motility function and parameter regime

The original Keller-Segel model (1.3) contains two independent parameters $\mu(v)$ and $\chi(v)$. Usually, they are taken as positive constants and hence the relation (1.6) fails. On the other hand, the model (1.1) is decided by the single choice of γ, and the relation (1.6) is automatically satisfied. Most information on the chemotactic behavior in the model is included in the motility function $\gamma(v)$ and hence, the critical step is how to choose the motility function. The motility function γ in (1.2) is general enough and provides all of the typical patterns in phase separation dynamics depending on the choice of the four coefficients, a, b, c, and d. We construct the nonlinear motility function γ from diffusion models with constant diffusivity.

Transition between active and inactive states. It is well-documented that exposure to a hormone may reduce the mobility of many organisms. Suppose that a cell becomes inactive with a small diffusivity $a > 0$ if exposed to the hormone. It becomes active with a larger diffusivity $a + b > 0$ if not exposed to the hormone for a while. Such a situation can be modeled by reaction-diffusion equations,

$$\begin{cases} \partial_t u_1 = a\Delta u_1 + \dfrac{1}{\delta}(k(v)u_2 - h(v)u_1), \\ \partial_t u_2 = (a+b)\Delta u_2 - \dfrac{1}{\delta}(k(v)u_2 - h(v)u_1), \\ \partial_t v = \varepsilon\Delta v + (u_1 + u_2) - v, \end{cases} \quad t \in (0,T),\ x \in \Omega, \tag{2.1}$$

where u_1 is the density of inactive cells with diffusivity $a > 0$, u_2 the density of active ones with a larger diffusivity $a + b$, and v the density of a signaling chemical (or hormone) produced by the cells. The function $h(v)$ is the conversion rate that inactive cells turns into active cells, which decreases as v increases. In other words, the chemical reduces cell motility. Similarly, the other conversion rate $k(v)$ is assumed to be an increasing function of v. In summary, we assume

$$h'(v) \le 0, \quad k'(v) \ge 0. \tag{2.2}$$

Funaki *et al.* [9] showed that, if the conversion rates h and k are smooth, and bounded above and below away from zero, then the total population density $u = u_1 + u_2$ and the chemical density v converge to the solution of

$$\begin{cases} u_t = \Delta(\gamma(v)u), \\ v_t = \varepsilon\Delta v + u - v, \end{cases} \quad t \in (0,T),\ x \in \Omega \tag{2.3}$$

as $\delta \to 0$, where

$$\gamma(v) = \frac{(a+b)h(v) + ak(v)}{h(v)+k(v)} = a + \frac{bh(v)}{h(v)+k(v)}.$$

If we choose

$$h(v) = \frac{1}{(1+v)^c} \quad \text{and} \quad k(v) = 1 - \frac{1}{(1+v)^c} \tag{2.4}$$

for an exponent $c > 0$, then (2.2) is satisfied and

$$\gamma(v) = a + \frac{b}{(1+v)^c}.$$

Then, $\gamma'(v) < 0$, $\gamma(v) \to a$ as $v \to \infty$, and $\gamma(v) \to a+b$ as $v \to 0$. The case $a = 0$ is the limit case that the slower cells do not diffuse at all, which allows the peak type solution. However, it is more natural to expect $a > 0$ in most cases. The motility function γ in (1.2) is a generalization of this case. See [9] for a rigorous convergence.

Bifurcation. Let $m = 1$ and $\mu_1 > 0$ be the principal eigenvalue of $-\Delta$ on the domain Ω under the Neumann boundary condition. If we linearize the system (2.3) at a constant equilibrium $(\bar{u}, \bar{v})$ with $\bar{u} = \bar{v}$, we obtain

$$\begin{cases} u_t = \gamma(\bar{v})\Delta u + \gamma'(\bar{v})\bar{u}\Delta v, \\ v_t = \varepsilon\Delta v + u - v, \end{cases} \quad t \in (0,T),\ x \in \Omega.$$

Therefore, the sign of eigenvalues of the matrix

$$\begin{bmatrix} -\gamma(\bar{v})\mu_1 & -\gamma'(\bar{v})\bar{u}\mu_1 \\ 1 & -\varepsilon\mu_1 - 1 \end{bmatrix}$$

determines the sign of eigenvalues of the linearized system above. Since the trace is negative, at least one of the eigenvalues is negative. The bifurcation curve surface is given when the determinant becomes zero, which is

$$\left(a + \frac{b}{(d+\bar{v})^c}\right)(\varepsilon\mu_1 + 1) - \frac{cb\bar{v}}{(d+\bar{v})^{c+1}} = 0.$$

If we write the equation for b, we obtain

$$b = \frac{-a(\varepsilon\mu_1+1)(d+\bar{v})^{c+1}}{(\varepsilon\mu_1+1-c)\bar{v} + (\varepsilon\mu_1+1)d}.$$

There are seven parameters, $a, b, c, d, \bar{v}, \varepsilon$, and μ_1. The principal eigenvalue μ_1 is a constant decided by the domain Ω. The other six parameters can be freely chosen.

In Figure 1, bifurcation curves are given for b and $\bar{v}$ when other coefficients are fixed as in the caption. We can see that the bifurcation curves converge to the purple-colored solid curve as $\varepsilon \to 0$. This is the curve that decides the excitable density set E when b is chosen. For example, if $b = 20$, the horizontal line segment between the curve for $\varepsilon = 0$ gives the excitable density set. Note that this set is bounded above and below away from zero. The segment between the curve for $\varepsilon = 0.01$ gives the range of steady state value $\bar{v}$ which are unstable when $\varepsilon = 0.01$. We can see the set expands as b increases and becomes empty if $b < 9$ in the figure.

In Figure 2, bifurcation curves are given for four different values of a. We can see that the excitable set E expands as a decreases. It looks like that the excitable set becomes unbounded as $a \to 0$, which will be confirmed in the next section.

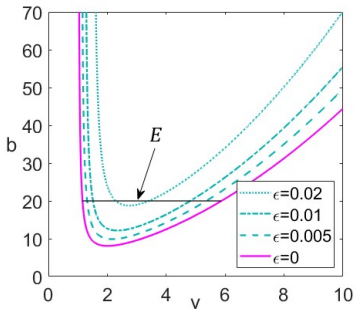

FIGURE 1. Bifurcation curves of (1.1) for the relation between b and $\bar{v}$. Other parameters are fixed at as $a = 0.3$, $\mu_1 = \pi^2$, $c = 2$, $m = 1$, and $d = 1$.

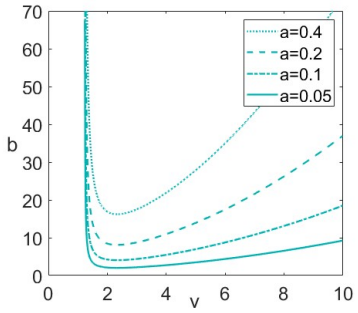

FIGURE 2. Bifurcation curves of (1.1) for the relation between b and $\bar{v}$. Other parameters are fixed at $\varepsilon = 0.01$, $\mu_1 = \pi^2$, $c = 2$, $m = 1$, and $d = 1$.

Similarly, we can find the bifurcation curve of constant equilibrium solution $(\bar{u}, \bar{v})$ of the reaction-diffusion system (2.1) with (2.4). In this system, the parameter d is set to be one and there is an extra parameter $\delta > 0$. The corresponding equation is

$$ABC - \frac{1}{\delta^2}k(\bar{v})\eta + \frac{1}{\delta^2}h(\bar{v})\eta + \frac{1}{\delta}A\eta - \frac{1}{\delta}B\eta - C\frac{1}{\delta^2}h(\bar{v})k(\bar{v}) = 0,$$

where

$$\begin{aligned} A &= -a\mu_1 - \frac{1}{\delta}h(\bar{v}), \\ B &= -(a+b)\mu_1 - \frac{1}{\delta}k(\bar{v}), \\ C &= -\varepsilon\mu_1 - 1, \\ \eta &= k'(\bar{v})h(\bar{v})\bar{v} - h'(\bar{v})k(\bar{v})\bar{v}. \end{aligned}$$

One can easily compute that the bifurcation curve converges to the ones for the problem (1.1) as $\delta \to 0$.

3. Aggregation viewed as an instability

Keller and Segel [14] viewed the initiation of slime mold aggregation as an instability of a constant steady state and we follow that in this section. Their main case can be written as

$$\begin{cases} u_t = \nabla \cdot \mu_0\big(\nabla u - \chi_0 \frac{u}{v}\nabla v\big), \\ v_t = \varepsilon \Delta v + u - v, \end{cases}$$

where μ_0 and χ_0 are constant. If $\bar{u} = \bar{v}$, the constant state $(\bar{u}, \bar{v})$ is a steady state and it is unstable if $\chi_0 > 1$. Note that the stability of a steady state is independent of the steady state itself for the classical logarithmic Keller-Segel equations. In contrast, in the case of (1.1), if $\bar{u}$ is too small or too large, $(\bar{u}, \bar{v})$ becomes a stable steady state as we will see in the section.

Denote the mean of the cell density by $\bar{u} = \frac{1}{|\Omega|}\int_\Omega u dx$. Then, a constant state $(\bar{u}, \bar{v})$ is a steady-state solution of (1.1) if and only if $\bar{v} = \bar{u}$. We call the mean density $\bar{u}$ (or $\bar{v}$) *excitable* if the chemosensitivity corresponding to the steady state is greater than 1, i.e., $\chi(\bar{v}) > 1$ for $\bar{v} = \bar{u}$. We denote the collection of excitable density values by

$$E = E_{\gamma,m} := \Big\{ v > 0 : \chi(v) = -\frac{v\gamma'(v)}{m\gamma(v)} > 1 \Big\} \tag{3.1}$$

and call it the excitable density set. The excitable density set is decided by the motility function γ and the nonlinearity $m > 0$. We will see that the shape of the excitable density set E decides the aggregation pattern types.

Lemma 3.1. *(i) If the excitable density set E contains an unbounded interval (i.e., $(v_0, \infty) \subset E$ for some $v_0 > 0$), then $a = 0$ and $c \geq m$. (ii) If E is bounded, then $a > 0$ or $c \leq m$, and peak solutions are not allowed.*

Proof. *(i)* Suppose that $(v_0, \infty) \subset E$ for some $v_0 > 0$. The relation to be an excitable density is written as $\frac{\gamma'(v)}{\gamma(v)} < \frac{-m}{v}$. Integrating it with respect to v gives

$$0 < \gamma(v) < Cv^{-m} \quad \text{for all} \quad v > v_0 \tag{3.2}$$

for some constant $C > 0$. Therefore, the decay of $\gamma(v) \to 0$ as $v \to \infty$ should be faster than or equal to the one of v^{-m}. This is possible only when $a = 0$ and $c \geq m$ for the motility functions given by (1.2).*(ii)* If E is bounded, any upper bound of E becomes a stable upper solution. This indicates that a peak solution may appear only when E is unbounded. □

We show that, if $\bar{u} = \bar{v} \in E$, and $\varepsilon > 0$ is small enough, the constant steady-state $(\bar{u}, \bar{v})$ is unstable.

Theorem 3.2 (Instability criterion)**.** *Let $\Omega \subset \mathbb{R}^n$ be a bounded smooth domain, $\mu_1 > 0$ be the principal eigenvalue of $-\Delta$ on Ω under the Neumann boundary condition, $\gamma(v) > 0$ be a smooth motility function defined on $\mathbb{R}^+$, and $(\bar{u}, \bar{v})$ be a constant steady-state solution of* (1.1)*. For an excitable density $\bar{v} \in E$, denote $\varepsilon_1(\bar{v}) := -\frac{1}{\mu_1}\Big(1 + \frac{\bar{v}\gamma'(\bar{v})}{m\gamma(\bar{v})}\Big)$. (i) If $0 < \varepsilon < \varepsilon_1$, $(\bar{u}, \bar{v})$ is linearly unstable. (ii) If $\varepsilon > \varepsilon_1(\bar{v})$, $(\bar{u}, \bar{v})$ is linearly stable. (iii) If $\bar{v} \notin E$, $(\bar{u}, \bar{v})$ is linearly stable for all $\varepsilon > 0$. (iv) If $E = \emptyset$, $(\bar{u}, \bar{v})$ is linearly stable for all $\bar{v} > 0$ and $\varepsilon > 0$.*

Proof. If $\bar{v} \in E$, we obtain $\varepsilon_1(\bar{v}) > 0$. Let $u = \bar{u} + u_1$ and $v = \bar{v} + v_1$. Then, the linearized problem of (1.1) at the steady-state $(\bar{u}, \bar{v})$ is given by

$$\frac{\partial}{\partial t}\begin{pmatrix} u_1 \\ v_1 \end{pmatrix} = \begin{pmatrix} m\gamma(\bar{v})\bar{u}^{m-1}\Delta & \bar{u}^m\gamma'(\bar{v})\Delta \\ 1 & \varepsilon\Delta - 1 \end{pmatrix}\begin{pmatrix} u_1 \\ v_1 \end{pmatrix} =: A(\bar{u}, \bar{v})\begin{pmatrix} u_1 \\ v_1 \end{pmatrix}. \tag{3.3}$$

Let (μ, ϕ) be an eigen-pair of the Laplace operator $-\Delta$ under the Neumann boundary condition and

$$B(\bar{u}, \bar{v}) := \begin{pmatrix} -m\gamma(\bar{v})\bar{u}^{m-1}\mu & -\bar{u}^m\gamma'(\bar{v})\mu \\ 1 & -\varepsilon\mu - 1 \end{pmatrix}.$$

Let $(\lambda, \mathbf{c})$ be an eigen-pair of the matrix B. Then,

$$A(\bar{u}, \bar{v})(\phi e^{\lambda t}\mathbf{c}) = B(\bar{u}, \bar{v})(\phi e^{\lambda t}\mathbf{c}) = \lambda\phi e^{\lambda t}\mathbf{c} = \frac{\partial}{\partial t}(\phi e^{\lambda t}\mathbf{c}),$$

and hence $\phi e^{\lambda t}\mathbf{c}$ is a solution of (3.3). Therefore, the sign of eigenvalues of B determines the local stability of constant steady-states. The characteristic equation of B is

$$\lambda^2 + (m\gamma(\bar{v})\bar{u}^{m-1}\mu + \varepsilon\mu + 1)\lambda + m\gamma(\bar{v})\bar{u}^{m-1}\mu(\varepsilon\mu + 1) + \bar{u}^m\gamma'(\bar{v})\mu = 0.$$

The eigenvalues are $\lambda_\pm := \frac{-P \pm \sqrt{P^2 - 4Q}}{2}$, where $P := m\mu(\gamma(\bar{v})\bar{u}^{m-1} + \varepsilon) + 1$ and $Q := \bar{u}^{m-1}[\varepsilon m\gamma(\bar{v})\mu^2 + (m\gamma(\bar{v}) + \bar{u}\gamma'(\bar{v}))\mu]$. Since P is positive, the steady-state $(\bar{u},\bar{v})$ is unstable if and only if there exists μ such that $Q(\mu) < 0$. Since $Q(\mu)$ takes its minimum value when $\mu = \mu_1$, and

$$\frac{Q(\mu_1)}{\bar{u}^{m-1}\mu_1} = \varepsilon m\gamma(\bar{v})\mu_1 + (m\gamma(\bar{v}) + \bar{u}\gamma'(\bar{v})) < 0$$
$$\iff \varepsilon < -\frac{1}{\mu_1}\Big(1 + \frac{\bar{v}}{m}\frac{\gamma'(\bar{v})}{\gamma(\bar{v})}\Big) = \varepsilon_1(\bar{v}).$$

Therefore, if $0 < \varepsilon < \varepsilon_1(\bar{v})$, $(\bar{u}, \bar{v})$ is linearly unstable, and if $\varepsilon > \varepsilon_1(\bar{v})$, $(\bar{u}, \bar{v})$ is linearly stable. If $\bar{v} \notin E$, $\varepsilon_1(\bar{v}) \le 0$. Therefore, for all $\varepsilon > 0$, $\varepsilon > \varepsilon_1$ and hence $(\bar{u}, \bar{v})$ is linearly stable. If $E = \emptyset$, $\varepsilon_1(\bar{v}) \le 0$ for any $\bar{v} > 0$. Hence, by the same reason, $(\bar{u}, \bar{v})$ is linearly stable for all $\bar{v} > 0$ and $\varepsilon > 0$. □

It is observed from several chemotaxis models that a minimum population size is required to make a cell aggregation start, which is called a critical mass phenomenon. This critical mass gives a necessary condition for aggregation, and the actual aggregation may happen depending on the initial distribution of the given mass (see [1]). In this section, we will see that the chemotaxis model (1.1) also has a related phenomenon in terms of density, not of the total mass. The phenomenon is divided into three cases. If $E = \mathbb{R}^+$, there is no critical density, which is the case of Keller-Segel equations. If $E = (v_0, \infty)$ as in (3.2), there is a critical density for the minimum density. If the excitable density set E is bounded, there are two critical densities for the lower and upper bound for the aggregation. We find E in the following theorems.

Theorem 3.3 ($a = 0$)**.** *Let γ be given by* (1.2)*, $a = 0$, and E the excitable density set* (3.1)*. (i) If $c > m$, then $E = (\frac{md}{c-m}, \infty)$. (ii) If $c \le m$, then $E = \emptyset$.*

Proof. Basically, we find the shape of the excitable density set E in this proof and the rest of the assertion of the theorem comes from Theorem 3.2. First, consider the case of $c > m$. Since $a = 0$, $v \in E$ if and only if

$$-\frac{v\gamma'(v)}{\gamma(v)} = c\left(\frac{v}{d+v}\right)\left(\frac{b}{a(d+v)^c+b}\right) = c\left(\frac{v}{d+v}\right) > m. \tag{3.4}$$

If we rewrite the inequality for v, we obtain

$$v > \frac{md}{c-m}.$$

Hence, the excitable density set is an unbounded open interval $E = (\frac{md}{c-m}, \infty)$. If $c \le m$, the inequality in (3.4) fails for any $v > 0$. Hence $E = \emptyset$. □

Next, let $a > 0$. Then, the condition to be an excitable density,

$$c\left(\frac{v}{d+v}\right)\left(\frac{b}{a(d+v)^c+b}\right) > m,$$

is equivalently written as

$$f(v) := m(v+d)^{c+1} + b(m-c)v/a + bdm/a < 0. \tag{3.5}$$

Hence, we may write $E = \{v \in \mathbb{R}^+ : f(v) < 0\}$.

Theorem 3.4 ($a > 0$)**.** *Let γ be given by (1.2), $f(v)$ by (3.5), $a > 0$, and*

$$\Lambda := \Big(\frac{c-m}{c+1}\Big)\Big(\frac{b(c-m)}{am(c+1)}\Big)^{1/c}. \tag{3.6}$$

(i) If $d < \Lambda$ and $c > m$, f has two zeros, $z_1 \ge 0$ and $z_2 > z_1$, and $E = (z_1, z_2)$. (ii) If $\Lambda < d$ or $c < m$, $E = \emptyset$.

Proof. The first and the second order derivatives of f in (3.5) are

$$\begin{aligned} f'(v) &= m(c+1)(v+d)^c + b(m-c)/a, \\ f''(v) &= mc(c+1)(v+d)^{c-1}. \end{aligned}$$

Since $f''(v) > 0$ for $v > 0$, f is a convex function on $\mathbb{R}^+$. Furthermore, since $f(0) = md^{c+1} + bdm/a \ge 0$, $\lim_{v\to\infty} f(v) = \infty$, and $E = \{v > 0 : f(v) < 0\}$, E is a nonempty set if and only if f has a negative minimum value at a critical point $\hat{v} > 0$. If $d = 0$, $f(0) = 0$ and hence $z_1 = 0$ is a zero of $f(v)$.

Let $\hat{v}$ be a positive critical value, i.e., $f'(\hat{v}) = 0$ and $\hat{v} > 0$. Then, it satisfies

$$(\hat{v}+d)^c = \frac{b(c-m)}{am(c+1)}.$$

Therefore, if $c \le m$, there is no such positive zero, and hence $E = \emptyset$. Suppose that $c > m$. Then, the critical point of f is unique and given by

$$\hat{v} := \left(\frac{b(c-m)}{am(c+1)}\right)^{1/c} - d,$$

and $f(v)$ has its minimum when $v = \hat{v}$. Compute that

$$f(\hat{v}) < 0 \iff d < \Big(\frac{c-m}{c+1}\Big)\Big(\frac{b(c-m)}{am(c+1)}\Big)^{1/c} = \Lambda.$$

Since $\left(\frac{c-m}{c+1}\right) < 1$, the condition $\Lambda > d$ implies $\left(\frac{b(c-m)}{am(c+1)}\right)^{1/c} > d$, i.e., $\hat{v} > 0$. Finally, since f is convex on $\mathbb{R}^+$, f has two positive zeros $0 < z_1 < z_2$. Therefore, E is a bounded open interval if and only if $d < \Lambda$. □

Cell aggregation usually starts when population size (or density) passes over a certain level. If the motility function γ is given by (1.2), the chemotaxis model (1.1) has the property when $a = 0$ and $c > m$. Then, the excitable density set E becomes an unbounded open interval $E = (\frac{md}{c-m}, \infty)$. Therefore, large population size is a key to aggregation. However, if $a > 0$, $c > m$, and $d < \Lambda$, the set E becomes a bounded interval $E = (z_1, z_2)$. Therefore, the population size should be in a reasonable range to get the aggregation started. Both too much and too little population are obstacles to aggregation which is biologically correct. On the other hand, if $d = 0$ and $a > 0$, we get $z_1 = 0$ and $z_2 = \left(\frac{p(c-m)}{m}\right)^{1/c}$, i.e., $E = (0, \left(\frac{p(c-m)}{m}\right)^{1/c})$. In this case, too large a population would be an obstacle to aggregation, but not too small.

4. Numerical Simulations

In this section, we numerically compute the chemotaxis model (1.1) in two space dimensions and test how aggregation patterns emerge and develop. We consider two cases of the motility function in (1.2), $a = 0$ and $a = 0.02$. The solution behavior given in Desvillettes *et al.* [7] is when $\gamma(v) = \frac{b}{d+v^c}$. This case corresponds to the case with $a = 0$ and we will see that the two are indistinguishable.

4.1. Cases with $a = 0$.

For a numerical simulation, we take a rectangular domain $\Omega = (0, 20) \times (0, 20)$ and parameters,

$$m = 2,\ c = 4,\ a = 0,\ b = 1,\ d = 0.5. \tag{4.1}$$

Then, $\frac{md}{c-m} = \frac{1}{2}$ and hence the excitable density set is $E = (\frac{1}{2}, \infty)$ by Theorem 3.3. We take initial values as

$$u(x, 0) = 1 \text{ and } v(x, 0) = 1 + X, \tag{4.2}$$

where X is a random variable with values $-0.05 \le X \le 0.05$. This initial value is a small perturbation of a constant steady state $(\bar{u}, \bar{v}) = (1, 1)$, which is unstable since $1 \in E$. The critical diffusivity is approximately $\varepsilon_1 = -\frac{1}{\mu_1}(1 + \frac{\bar{v}\gamma'(\bar{v})}{m\gamma(\bar{v})}) \cong 13.51$, where μ_1 is the principle eigenvalue of the Laplace operator $-\Delta$ on the given domain under the Neumann boundary condition. We take the diffusivity ε of the signaling chemical as $\varepsilon = 0.05 < \varepsilon_1$. Therefore, the instability conditions are satisfied, and hence, cells are expected to aggregate by Theorem 3.3. Note that, since $\frac{\varepsilon_1}{\varepsilon}$ is large, a large number of aggregation spots appear initially.

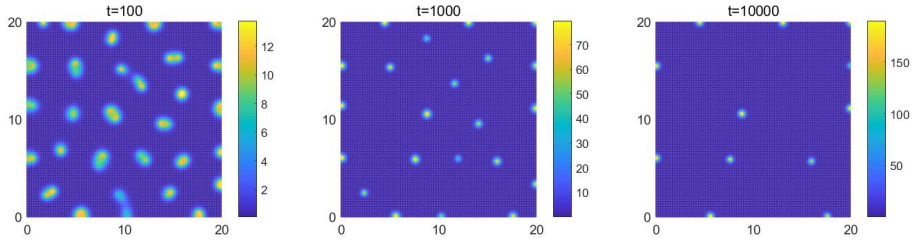

Figure 3. Snap shots of the numerical solution for the cell density u. If γ is given by (1.2) with $a = 0$, it gives cell aggregation peaks.

In Figure 3, three snapshots of a numerical solution of (1.1) are given when the parameters and initial values are given in (4.1) and (4.2). Only the images of the population density u are given at three different moments $t = 10^2, 10^3$, and 10^4. In the first figure at the moment $t = 10^2$, we see many spots of density 13 or less. Some of them are stuck together like Siamese twins, which are about to be merged into a single spot. As time increases, the number of spots decreases, and the density of spots increases. However, the radius of each peak changes little. The patterns in Figure 3 can be called hot spots since the density inside the spot takes higher values. However, since the height keeps increasing as spots are merged, it is rather called a peak. This is the typical behavior of peak solutions. This solution behavior is similar to the one in Desvillettes *et al.* [7, Figure 4.5].

4.2. **Case with $a > 0$.** The peak solutions are well-known patterns in chemotaxis models. Patterns such as hot spot, cold spot, and stripe patterns are well-known in phase separation models and in Turing patterns. It is a new observation that the chemotaxis model such as (1.1) also produces such patterns.

The critical value $\Lambda := \left(\frac{c-m}{c+1}\right)\left(\frac{b(c-m)}{am(c+1)}\right)^{1/c}$ in Theorem 3.4 depends on four parameters. We fix three of them as

$$m = 2,\ c = 4,\ a = 0.02,$$

and treat Λ as a function of b. In Figure 4, the graph of the function is given in the plane of d and b variables, i.e., $d = \Lambda(b)$. If $d = 1$ and $b = 1$, then $d > \Lambda(b)$ and the excitable density set E becomes empty by Theorem 3.4. The graph of the convex function $f(v)$ in (3.5) is given in Figure 4. We can confirm that $f > 0$ for all $v > 0$ and hence $E = \emptyset$. In this case, all constant steady-states are stable and we do not expect any pattern formation.

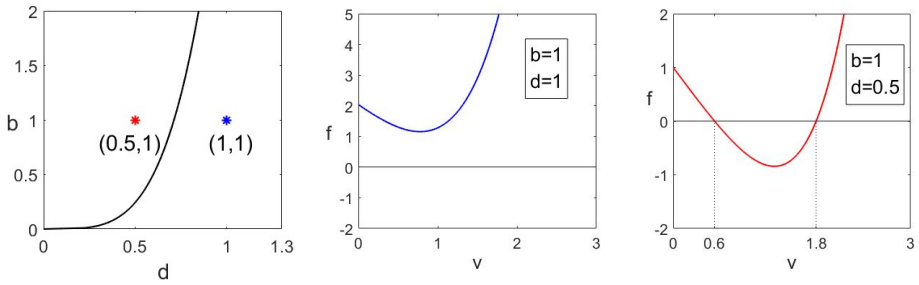

FIGURE 4. **(Graphs of Λ and $f(v)$)** Parameters are $m = 2, c = 4, a = 0.02$.

In the second example, we take $d = 0.5$ and $b = 1$ so that $d < \Lambda(b)$. The graph of the convex function $f(v)$ for this case is given in Figure 4. We can see that $f(v) < 0$ for $v \in E \cong (0.6, 1.8)$. Therefore, if $\bar{v} \in E$, we may expect a pattern formation when $\varepsilon > 0$ is small enough. To compute the solution of (1.1) with the motility function (1.2), we take the example of the previously discussed one with the same parameter values,

$$m = 2,\ c = 4,\ a = 0.02,\ b = 1,\ d = 0.5, \tag{4.3}$$

and a larger domain

$$\Omega = (0, 100) \times (0, 100).$$

We take the same initial values as

$$u(x, 0) = 1, \text{ and } v(x, 0) = 1 + X, \quad x \in \Omega,$$

where X is the same random variable which takes values $-0.05 \leq X \leq 0.05$. The initial value is a perturbation of a constant steady-state $(\bar{u}, \bar{v}) = (1, 1)$ and $1 \in E$. In this case, the critical diffusivity is $\varepsilon_1 \cong 213.53$. We take $\varepsilon = 0.05 < \varepsilon_1$ and hence, an aggregation phenomenon is expected.

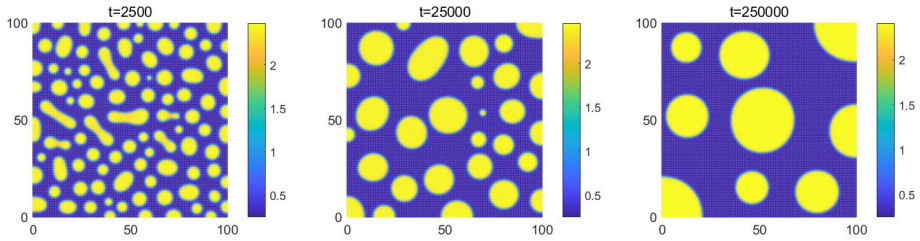

FIGURE 5. Snap shots of cell density u. Hot spots are observed when $\bar{u} = 1$. Motility γ is by (1.2) and parameters are in (4.3).

In Figure 5, three snapshots of the population density u are given at three different moments $t = 2500, 25000$, and 250000. There are lots of spots at the moment of $t = 250$. As time passes, the spots are merged together and make larger spots. The difference in comparison with the ones in Figure 3 is that the area of the circular domain increase, but their height is not changing. Hence, the spot is more like a plateau. This pattern is similar to the hot spots of Turing patterns. The difference is that the spot size is uniform for a Turing pattern. However, the size of hot spots in Figure 5 varies a lot. In reality, the size of slugs in amoeba cell aggregates is not uniform and varies greatly, which is similar to the figure. The patterns in Figure 5 are approximately bounded approximately between $u = 0.3$ and 2.4.

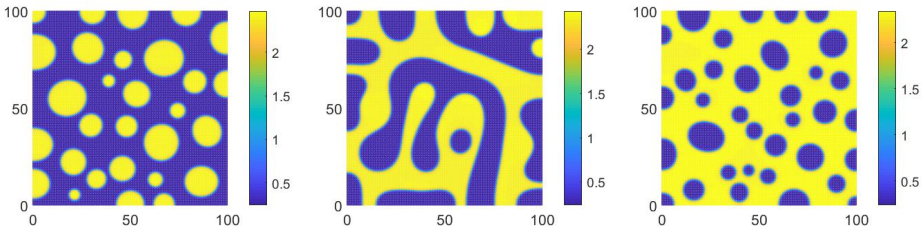

FIGURE 6. Various patterns appear depending on the mean population density, which are $\bar{u} = 1, 1.3$, and 1.7 from the left.

If the population density changes, various patterns appear. These patterns fall into three categories, which are compared in Figure 6. The first figure is from Figure 3, which is for hot spots. The second figure is a stripe pattern obtained when the initial population is $\bar{u} = 1.3$. Roughly speaking, if there is too much population and there is no enough space, the hot spots are connected and form stripes. If the

initial population is increased to $\bar{u} = 1.7$, the stripe patterns turn into cold spots as in the third figure in Figure 6. These patterns are like sinkholes with flat bottoms, where the lower population density exists only inside spots.

5. Aggregation viewed as a phase separation

In this section, we consider the elliptic problem,

$$\begin{cases} 0 = (\gamma(v)u^m)_{xx}, & 0 < x < \ell, \\ 0 = \varepsilon v_{xx} - v + u, & 0 < x < \ell, \\ \partial_x u = \partial_x v = 0, & x = 0 \text{ and } \ell, \end{cases} \tag{5.1}$$

where $m > 0$ and $\varepsilon > 0$. This problem is satisfied by the steady state solution of the chemotaxis model (1.1) in one space dimension. Nonconstant solutions of the elliptic problem reflect aggregation patterns observed numerically. The motility function γ and the parameter regimes in the section are

$$\gamma(v) = a + \frac{b}{(d+v)^c}, \quad a, b > 0,\ c > m,\ 0 \le d < \Lambda, \tag{5.2}$$

where

$$\Lambda = \Big(\frac{c-m}{c+1}\Big)\Big(\frac{b(c-m)}{am(c+1)}\Big)^{1/c}.$$

The parameter regime above is the one in Theorem 3.4 that gives a non-empty excitable set, $E \neq \emptyset$, and uniformly bounded cell aggregation patterns. In this section, we employ the phase separation theory of Carr, Gurtin, and Slemrod [2] to characterize the pattern formation. We consider the case when $a > 0$. The aggregation pattern is studied well in the other cases. It has been shown that the solution u and v are of peak type with spikes at the boundary $x = 0$ or $x = \ell$ when $\frac{\gamma'(v)v}{m\gamma(v)} < 1$ for all $v \in \mathbb{R}^+$, i.e., when $E = (0, \infty)$ (see [7, 22]). The motility function in (5.2) satisfies the condition when $a = 0, d = 0$, and $c > m$.

Recall that the *excitable density set* E is given by

$$E := \Big\{ v > 0 : -\frac{\gamma'(v)v}{m\gamma(v)} > 1 \Big\}.$$

A constant state $(\bar{u}, \bar{v})$ is a solution of (5.1) if $\bar{u} = \bar{v}$. If $\bar{v} \in E$, this constant solution is unstable and the evolution problem (1.1) will develop a pattern starting from the unstable steady state after a small perturbation. For a non-constant static solution (u, v) of (5.1), the two components u and v don't need to be identical. However, they have the same mass, i.e.,

$$\bar{u} = \frac{1}{\ell}\int_0^\ell u dx = \frac{1}{\ell}\int_0^\ell (v - \varepsilon v_{xx}) dx = \frac{1}{\ell}\int_0^\ell v dx = \bar{v},$$

by the second equation of (5.1) and the boundary condition. The existence of a nonconstant monotone solution with mean

$$\frac{1}{\ell}\int_0^\ell v(x) dx = \bar{v} \tag{5.3}$$

has been proved by Wang and Xu [22, Theorem 2.1] when $m = 1$ and $\bar{v} \in E$. The proof can be extended to the case with $m > 0$ easily. However, the set E is not the maximal set that gives a pattern. In this section, we find the maximal interval (α, β) that includes E using the phase separation theory.

First, consider a function,

$$g(v) := \gamma(v)^{-1/m} = \frac{(d+v)^{c/m}}{(a(d+v)^c + b)^{1/m}}. \tag{5.4}$$

The function $g(\cdot)$ is smooth and satisfies the four properties in the following lemma.

Lemma 5.1. *If $a, b > 0$, $c > m$, and $0 \le d < \Lambda$, then*

- A1. *$g_0 \le g(v) < M$ for $g_0 = \frac{d^{c/m}}{(ad^c+b)^{1/m}} (= g(0))$ and $M = a^{-\frac{1}{m}} (= \lim_{v\to\infty} g(v))$,*
- A2. *$g'(v) > 0$ for all $v > 0$.*
- A3. *There is $v_c > 0$ such that $g''(v) > 0$ for $0 < v < v_c$, $g''(v) < 0$ for $v > v_c$, and $g'(v_c) > \frac{g(v_c)}{v_c}$.*
- A4. *There exists a unique constant $K_0 > 0$ such that*
  - (a) *$K_0 g(v) - v$ has three zeros, $0 < \alpha < \mu < \beta$,*
  - (b) *$K_0 g(v) - v > 0$ in $[0, \alpha) \cup (\mu, \beta)$ and $K_0 g(v) - v < 0$ in $(\alpha, \mu) \cup (\beta, \infty)$, and*
  - (c) *$\int_\alpha^\beta (K_0 g(s) - s) ds = 0$.*

Proof. The first two properties, A1 and A2, are satisfied directly from the function $g(v)$ in (5.4) for even without the restrictions of the parameters. The property A4 directly comes from A3. We only need to show A3. By computation, we can find that the inflection point of $g(v)$ is

$$v_c = \left(\frac{b(c-m)}{am(1+c)}\right)^{1/c} - d.$$

Since $d < \Lambda$ and $\frac{c-m}{c+1} < 1$, we ave $v_c > 0$. One can algebraically check

$$g'(v_c) > \frac{g(v_c)}{v_c} \iff -\frac{\gamma'(v_c)v_c}{m\gamma(v_c)} > 1 \iff v_c \in E.$$

Notice that the two conditions $d < \Lambda$ and $v_c \in E$ are equivalent as proved in Theorem 3.4, which completes the proof. □

We deduce from A4 that $K_0 g'(\alpha) < 1$ and $K_0 g'(\beta) < 1$. The graph of the difference $y = K_0 g(v) - v$ is given in Figure 7 when the parameters in (4.3) are used. In this example, the numerical values are

$$K_0 = 0.1957, \quad \alpha = 0.244, \quad \mu = 1.32, \quad \beta = 2.381.$$

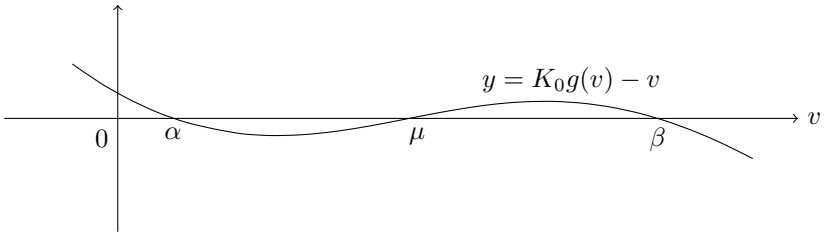

FIGURE 7. Graph of $K_0 g(v) - v$. $a = 0.02$, $b = 1$, $c = 4$, $d = 0.5$, $m = 2$, and $K_0 = 0.1957$. Here, $\alpha \approx 0.244, \mu \approx 1.32, \beta \approx 2.381$.

Next, we decouple u and v. Integrating the first equation of (5.1) twice using the homogeneous Neumann boundary condition gives

$$\gamma(v)u^m = K^m$$

for a constant $K > 0$. We have the freedom to choose K. For a constant solution case $(\bar{u}, \bar{v})$, we have $\bar{u} = \bar{v}$ and K is given by

$$K = \sqrt[m]{\gamma(\bar{v})\bar{v}^m}.$$

However, the constant solution is not stable for $\bar{v} \in E$ and we can observe only non-constant solutions in numerical computations. To obtain a non-constant solution case, we have to choose $K = K_0$, the unique constant in the property A4 in Lemma 5.1. This is needed since the Maxwell line of van der Waals' double well potential should be taken as explained below. Then, the mass condition (5.3) is satisfied by the profile (or the interface for the case of $\varepsilon \to 0$ limit) of the solution. Since we observe stable nonconstant patterns, we explore the case $K = K_0$ and rewrite the relation as

$$u = K_0 g(v). \tag{5.5}$$

If we put (5.5) into the second equation of (5.1), we obtain a decoupled problem,

$$\begin{cases} \varepsilon v_{xx} + K_0 g(v) - v = 0 & \text{in } (0, \ell), \\ v_x(0) = v_x(\ell) = 0. \end{cases} \tag{5.6}$$

We are ready to construct a minimization problem for the phase separation which takes (5.6) as its Euler-Lagrange equation. We briefly introduce the theory from [2]. Let $W(\cdot)$ be a double-well potential. It is assumed to satisfy the properties below;

B1. $W : (0, \infty) \to \mathbb{R}$ is C^5,
B2. $W'' > 0$ on $(0, w_1) \cup (w_2, \infty)$, and $W'' < 0$ on (w_1, w_2) for some w_1, w_2,
B3. $W'(0) < W'(w_2)$, $W'(\infty) > W'(w_1)$.

Let $H^1(0, \ell)$ be the usual Sobolev space of square-integrable functions possessing square-integrable first derivatives, and $H^1_+(0, \ell)$ be its subcollection with positive functions. The energy of a function $w \in H^1_+(0, \ell)$ is defined as

$$\Psi(w) = \int_0^\ell \frac{1}{2}\varepsilon w'(x)^2 + W(w(x))dx,$$

where $\varepsilon > 0$ is small. The function $W(w)$ is the free energy per unit volume when the density is constant. The term $\varepsilon w'(x)^2$ accounts for the interfacial energy. The energy minimizer $v \in H^1_+(0, \ell)$ for a given mass $\bar{v} > 0$ is a function with the smallest energy, i.e.,

$$\Psi(v) \le \Psi(w) \ \text{ for all } \ w \in H^1_+(0, \ell) \ \text{ with } \ \frac{1}{\ell}\int_0^\ell w(x)dx = \bar{v}. \tag{5.7}$$

The following theorem for the existence, uniqueness, and solution structure of the minimizer is from Carr *et al.* [2].

Theorem 5.2 (Carr, Gurtin, and Slemrod [2])**.** *Let $0 < \alpha < \beta$ and satisfy*

$$W(\beta) - W(\alpha) = \sigma(\beta - \alpha) \ \text{ and } \ W'(\alpha) = W'(\beta) = \sigma \tag{5.8}$$

for some σ (see Figure 8). If $\varepsilon > 0$ is small enough and $\bar{v} \in (\alpha, \beta)$, the minimization problem (5.7) *has a unique (modulo reversal) global minimizer v_ε. In addition, v_ε*

is strictly monotone. Furthermore, as $\varepsilon \to 0$, v_ε *approaches a piece-wise constant solution* v_0 *given by*

$$v_0(x) = \begin{cases} \alpha, & 0 \le x < \ell_1 \\ \beta, & \ell_1 < x \le \ell, \end{cases}$$

where $\ell_1 = \frac{\ell(\beta - \bar{v}/\ell)}{\beta - \alpha}$. *If* $\bar{v} \notin (\alpha, \beta)$, *there is no such minimizer.*

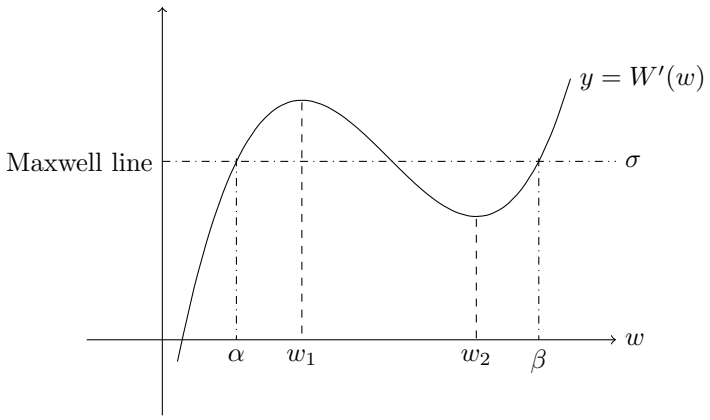

FIGURE 8. The two areas bounded by the Maxwell line $y = \sigma$ and the graph $y = W'$ have the same size.

The function $g(v)$ in (5.4) satisfies the four properties A1–A4 in Lemma 5.1 if the motility is given by (5.2). We take the potential as

$$W(w) = \int_0^w (s - K_0 g(s))ds, \tag{5.9}$$

where $K_0 > 0$ is the unique constant in A4. Then, W satisfies the three properties B1–B3. The condition (5.8) is satisfied with the same α and β in Property A4 and with $\sigma = 0$. Therefore, the corresponding Euler-Lagrange equation is (5.6). In other words, if v_ε is the unique minimum energy solution and $u_\varepsilon = K_0 g(v_\varepsilon)$, then $(u_\varepsilon, v_\varepsilon)$ is the steady state solution of (5.1).

Theorem 5.3. *Let* $\gamma(v)$ *be the motility function given by* (5.2). *There exist* $\alpha, \beta > 0$ *such that for any* $\bar{v} \in (\alpha, \beta)$ *and* $\varepsilon > 0$ *small enough, there exists a nonconstant monotone solution* $(u_\varepsilon, v_\varepsilon)$ *of* (5.1) *such that*

$$\alpha \le u_\varepsilon, v_\varepsilon \le \beta,$$

and

$$\lim_{\varepsilon \to 0} u_\varepsilon = \lim_{\varepsilon \to 0} v_\varepsilon = \begin{cases} \alpha, & 0 \le x \le \ell_1 \\ \beta, & \ell_1 < x \le \ell, \end{cases} \tag{5.10}$$

where $\ell_1 = \frac{\ell(\beta - \bar{v}/\ell)}{\beta - \alpha}$.

Proof. For the motility function γ in (5.2), the function $g(v) = \gamma(v)^{-1/m}$ satisfies the properties A1–A4 in Lemma (5.1). If we take the double-well potential W in (5.9) with the K_0 in A4, it satisfies B1–B3. The conditions in Theorem 5.2 are satisfied with the α and β in A4 and $\sigma = 0$. Hence, we may apply Theorem 5.2 for

$\varepsilon > 0$ small enough. Let $\bar{v} \in (\alpha, \beta)$ and v_ε be the minimum energy solution. Then, v_ε is monotone and satisfies (5.6). Denote $u_\varepsilon := K_0 g(v_\varepsilon)$. Then, u_ε is a composition of two monotone functions and hence is monotone. Since $\gamma(v_\varepsilon)u_\varepsilon^m = K_0^m$, the first equation of (5.1) is satisfied. Therefore, $(u_\varepsilon, v_\varepsilon)$ is a monotone solution of (5.1). To show the uniform bound of the solution, consider the case when v_ε is decreasing. Since v_ε has the maximum at $x = 0$ and satisfies the Neumann boundary condition, $\varepsilon v_\varepsilon''(0) \le 0$. Suppose that $v_\varepsilon(0) > \beta$. Then, $K_0 g(v_\varepsilon(0)) - v_\varepsilon(0) < 0$. It fails (5.6). Therefore, $v_\varepsilon(0) \le \beta$. Similarly, $v_\varepsilon(\ell) \ge \alpha$ and hence $\alpha \le v_\varepsilon(x) \le \beta$ for all $x \in (0, \ell)$. Since $\alpha = K_0 g(\alpha) \le K_0(g(v_\varepsilon(x)) = u(x) \le K_0 g(\beta) = \beta$, u_ε is also bounded by $\alpha \le u_\varepsilon(x) \le \beta$ for all $x \in (0, \ell)$. □

There could be many stationary solutions of the system (5.1). However, the minimum energy solution is monotone and bounded by α and β if ε is small enough. Since the solution converges to a step function given in (5.10), the minimum energy solution for small $\varepsilon > 0$ is given as in Figure 9. This minimum energy solution is stable. There could be other stationary solutions of (5.1). The patterns observed in Figures 5 and 6 represent such solutions in two space dimensions. However, they are unstable and what we can observe numerically is that they evolve slowly towards the minimum energy solution.

FIGURE 9. Single-layer plateau

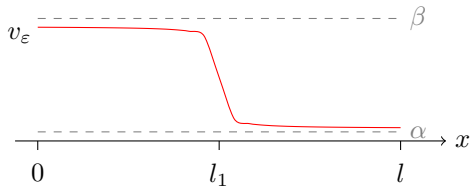

Chemotactic cell aggregation has been viewed in two ways, instability, and phase separation. Instability analysis shows the possibility of pattern formation, but not the shape. On the other hand, the phase separation theory explains the pattern shape quite in detail. Now we compare the two approaches.

Lemma 5.4. *(i) If $E = \emptyset$, then there is no such α, β in Theorem 5.3. (ii) If $E = (z_1, z_2)$ for some $z_1 < z_2$, $z_1, z_2 \in (\alpha, \beta)$.*

Proof. We may algebraically check the equivalence of

$$E = \emptyset \iff g'(v) \le \frac{g(v)}{v} \text{ for all } v > 0. \tag{5.11}$$

(*i*) We suppose $E = \emptyset$ and show $Kg(v) - v$ has at most one sign change for any given $K > 0$. Let $z > 0$ be a zero of $f(v) := Kg(v) - v$. Then, (5.11) implies

$$f'(v) = Kg'(v) - 1 \le \frac{Kg(v) - v}{v} = \frac{f(v)}{v}.$$

Suppose that $f(v_0) < 0$ for some $v_0 > 0$. Then, $f'(v_0) < 0$. Since f decreases when $f(v) < 0$, there is no chance to obtain a positive value $f(v) > 0$ for $v > v_0$. Hence, $f(v)$ may have a single sign change at most if $E = \emptyset$. Hence, $f(v)$ cannot be a balanced bistable nonlinearity.

(*ii*) Next, we show if $E \neq \emptyset$ and $E = (z_1, z_2)$ for some $z_1 < z_2$, then $z_1, z_2 \in (\alpha, \beta)$. Notice that z_1, z_2 are points which satisfy

$$g'(z_i) = \frac{g(z_i)}{z_i}, \quad i = 1, 2$$

(see Figure 10). Then, there exists $K_0 > 0$ that satisfies

$$g'(z_1) = \frac{g(z_1)}{z_1} < \frac{1}{K_0} < \frac{g(z_2)}{z_2} = g'(z_2)$$

so that $K_0 g(v) - v$ has three zeros α, μ, β with an order $\alpha < \mu < \beta$, and $\int_\alpha^\beta (K_0 g(v) - v) dv = 0$. Then, the graph of the function $K_0 g(v) - v$ corresponds to Figure 7. Since $K_0 g(z_1) - z_1 < 0$, we have $z_1 > \alpha$. Likewise, $K_0 g(z_2) - z_2 > 0$ implies $z_2 < \beta$. □

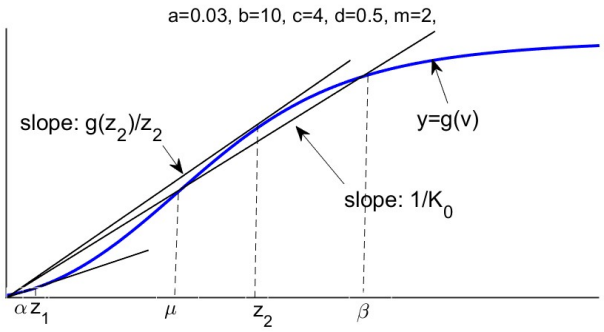

FIGURE 10. Relation among $\alpha, \mu, \beta, z_1, z_2$ and graph of $g(x)$.

Theorem 5.3 and Lemma 5.4 implies that there is an interesting situation that both constant and nonconstant steady states are stable. Hence, depending on the perturbation, the solution of the parabolic problem may converge to any of the two.

Corollary 5.5. *Let $\bar{v} \in (\alpha, z_1) \cup (z_2, \beta)$. (i) The constant state $(\bar{u}, \bar{v})$ is a stable solution of (1.1) if $\bar{u} = \bar{v}$. (ii) The minimal energy solution satisfying $\frac{1}{\ell}\int_0^\ell u dx = \bar{v}$ is nonconstant, monotone, and stable.*

6. Discussion and conclusion

The formation of patterns has attracted the attention of many theoretical and mathematical biologists. Reaction-diffusion equations have been used the most as mathematical models for the phenomenon, where the Turing patterns are the most famous [21] (see [5]). In these models, the population growth is modeled by reaction and the spreading by diffusion. Then, the patterns appear due to the balance between reaction and diffusion. However, in many cases, patterns appear without any population growth. Chemotactic cell aggregation is such a case. If food dwindles, amoeba starts to aggregate. Therefore, the main question is whether diffusion (or migration) alone can create aggregation patterns. In the paper, we have observed four aggregation patterns of the chemotactic self-organization model (1.1)–(1.2). If $a = 0$, the peak solutions are obtained, which are bounded for a fixed $\varepsilon > 0$ and blow up as $\varepsilon \to 0$.[1] If $a > 0$, the motility function γ has a positive lower bound,

[1]On the other hand, the solutions of the minimal model blow up in a finite time (see [12]) for a fixed $\varepsilon > 0$.

and patterns are uniformly bounded with respect to $\varepsilon > 0$. We have observed three classical Turing patterns depending on the initial mean population, stripes, hot spots, and cold spots. However, unlike the Turing patterns, the pattern size varies as in Figure 5, which agrees with the actual observation of amoeba slugs.

The global existence of the logarithmic Keller-Segel equation is obtained only for the parameter regimes without cell aggregation. Recently, Desvillettes *et al.* [7] and Winkler [23] showed global existence for the problem (1.1) in some parameter regimes with cell aggregation. The stability analysis in the paper shows that the global existence is still missing for a large portion of parameter regimes with cell aggregation. The main difficulty of the analysis comes from the degeneracy of the motility. Hence, the case with $a > 0$ gives the global existence more easily and makes aggregation patterns physically more meaningful.

The contribution of the paper from the technical side is that the technique of phase separation is introduced to the chemotaxis theory. The cell aggregation has been viewed as an instability of a constant steady state ever since Keller and Segel [14]. In particular, the cell aggregation patterns were peak types (see [17, 19]). These peak types solutions cannot be considered as a phase separation phenomenon. However, if the motility γ has a positive lower bound, which is physically meaningful as discussed in Funaki *et al.* [9] and Section 2, two phases appear, and the solution takes the two phases and the transition layer. This behavior allowed us to use the phase separation theory of Carr, Curtin, and Slemrod [2] and obtain the pattern formation in a wider range of density $\bar{v} \in (\alpha, \beta)$ together with the detailed structure of the solution. However, the analysis in the paper is for the one space dimension and needs to be done in multiple dimensions.

Appendix A. Symmetric versus random dispersal

In this section, we see that Fick's diffusion law in a heterogeneous environment is not for random dispersal. It is actually a symmetric dispersal whatever it means. To view the heterogeneous diffusion models clearly, we consider dispersal on a lattice. Let u_i be the population (or probability) at the ith patch. Denote c_{ij} $(= c_{i\leftarrow j})$ as the migration rate from patch j to patch i. Then, the rate of change of population u_i satisfies

$$\dot{u}_i = c_{ii-1}u_{i-1} + c_{ii+1}u_{i+1} - c_{i-1i}u_i - c_{i+1i}u_i. \tag{A.1}$$

There are two special dispersal relations. If $c_{ii+1} = c_{i+1i}$, i.e., if the migration rate of population from patch i to $i+1$ is equal to that from patch $i+1$ to i, the dispersal model (A.1) is called *symmetric* (see [16]). If we denote $\gamma_{i+1/2} := c_{ii+1} = c_{i+1i}$, (A.1) is rewritten as

$$\begin{aligned}\dot{u}_i &= \gamma_{i+1/2}(u_{i+1} - u_i) - \gamma_{i-1/2}(u_i - u_{i-1}) \\ &\cong \gamma_{i+1/2}u'_{i+1/2} - \gamma_{i-1/2}u'_{i-1/2} \\ &\cong (\gamma u')'_i.\end{aligned}$$

In the above approximation, the distance between two adjacent patches is assumed to be 1, which is considered small enough. In multi-space dimensions, this relation is written as a partial differential equation (PDE),

$$u_t = \nabla \cdot (\gamma(x)\nabla u),$$

which is called Fick's diffusion law. In other words, we may say that Fick's diffusion law is related to the symmetric dispersal on a patch system. However, the physical meaning of symmetric dispersal is not clear.

We are more interested in the case when $c_{i-1i} = c_{i+1i}$, i.e. when the migration rate from patch i to $i-1$ is equal to the one from patch i to $i+1$. This is the case that the probabilities to move to the right patch and the left one are identical and hence we may call it a *random* dispersal. If we denote $\gamma_i := c_{i+1i} = c_{i-1i}$, (A.1) is written as

$$\dot{u}_i \;=\; \gamma_{i-1}u_{i-1} + \gamma_{i+1}u_{i+1} - 2\gamma_i u_i \;\cong\; (\gamma u)_i''.$$

The corresponding PDE model in multi-space dimensions is

$$u_t = \Delta(\gamma(x)u),$$

which is the diffusion model used in the model of the paper (1.1). The physical meaning of this diffusion is random dispersal. Since this type of diffusion contains an advection phenomenon, it is often called a Fokker-Planck type diffusion.

Appendix B. Nonconstant static pattern and Maxwell line

We formally describe what dynamics in the chemotaxis model (1.1) create cell aggregation patterns. The instability analysis has been considered for a long time in chemotaxis theory and gives localized viewpoint. In the paper, we introduced a new approach based on the phase separation which gives a nonlocal viewpoint. We want to know the time asymptotic of the solution u under the zero-flux boundary condition. Since the total population is conserved, we have a restriction

$$\int_\Omega u(x,t)dx = \int_\Omega u(x,0)dx = \bar{u}|\Omega|,$$

where $\bar{u}$ is the average population. The asymptotic convergence of the aggregation pattern will satisfy the elliptic equation (5.1). The Neumann boundary condition for v and the second equation of (5.1) imply

$$\bar{v}|\Omega| = \int_\Omega v(x)dx = \int_\Omega \varepsilon\Delta v + u(x)dx = \bar{u}|\Omega|. \tag{B.1}$$

Under the zero-flux boundary condition, the first equation gives

$$\gamma(v)u^m = K^m, \quad K > 0, \tag{B.2}$$

where K is a constant free to choose. We need this freedom to fit the constraint (B.1).

The solution of (5.1) is not unique even under the constraint (B.1). The first group of solutions are constant ones. Constant solutions should have the mean value and hence $\bar{u} = \bar{v}$ and $(\bar{u}, \bar{v})$ is the constant solution. Hence, the constant K is given by $K = \Psi(\bar{u}, \bar{v})$. Note that we can always find a constant solution by taking this K. However, the instability analysis shows that some of them are unstable. In that case, we expect a nonconstant stable solution. Even if the constant solution is stable, we may still find a stable nonconstant solution.

Suppose that (u, v) is a nonconstant solution. Then, the relation (B.2) gives $u = Kg(v)$ with $g(v) = \gamma(v)^{-1/m}$. Then, we obtain a decoupled equation with v

only,

$$\begin{cases} 0 = \varepsilon\Delta v + Kg(v) - v & \text{in } \Omega \\ 0 = \partial_\nu v & \text{on } \partial\Omega. \end{cases} \tag{B.3}$$

Hence, finding a nonconstant solution of (5.1) is now turned to finding a nonconstant solution of (B.3). However, to obtain a nonconstant solution of (B.3), the reaction part $f(v) := Kg(v) - v$ should be a balanced bistable nonlinearity, i.e., there should exist two stable states, $\alpha < \beta$, and $\int_\alpha^\beta f(v)dv = 0$. In general, the reaction term does not satisfy the condition, but there may exist such a constant K depending on the function $g(v) = \gamma(v)^{-1/m}$. In Figure 11, the graphs of $y = g(v)$ are given for three cases together with graphs of $y = v/K$. If they can intersect each other at three points, there is such a case. The graph of $g(v)$ in the left is concave and hence there is no chance. The graph of the middle one has an inflection point, but there is no such a case. However, the right side one has three intersection point and we can find a K_0 such that $K_0 g(v) - v$ is a balanced bistable nonlinerity. If $K = K_0$ is chosen, then we may apply the phase separation theory with van der Waals' double-well potential $W(v) = -\int_0^v f(s)ds$, and $W' = 0$ becomes the Maxwell line. Such a constant K_0 is unique proved in Lemma 5.1. The overall shapes of the three cases in Figure 11 are not different much. However, subtle differences in the function $g(v) = \gamma(v)^{-1/m}$ make the aggregation patterns emerge.

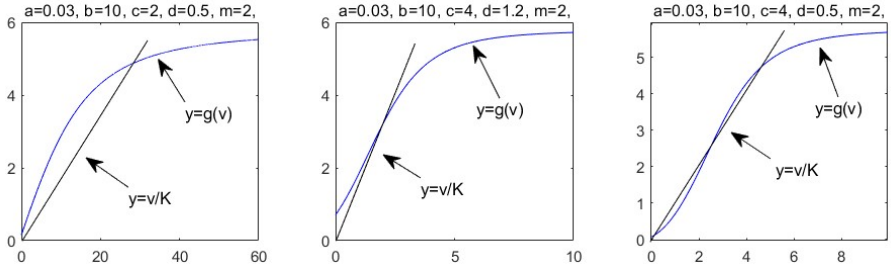

FIGURE 11. If there exists $K > 0$ such that the line $y = v/K$ intersects the graph of $y = g(v)$ three times, aggregation may occur.

Acknowledgments. This research was supported in part by National Research Foundation of Korea (NRF-2017R1A2B2010398).

REFERENCES

[1] A. Blanchet, J. A. Carrillo, and Ph. Laurençot, Critical mass for a Patlak-Keller-Segel model with degenerate diffusion in higher dimensions, Calc. Var. Partial Differential Equations 35 (2009), 133–168.

[2] J. Carr, M.E. Gurtin, and M. Slemrod, Structured phase transitions on a finite interval, Arch. Rational Mech. Anal. 86, (1984)

[3] B. Choi and Y.-J. Kim, Diffusion of biological organisms : Fickian and Fokker-Planck type diffusions, SIAM J. Appl. Math. 79 (2019) no.4, 1501-1527.

[4] E. Cho and Y.-J. Kim, Starvation driven diffusion as a survival strategy of biological organisms, Bull. Math. Biol. 75 (2013), 845–870.

[5] J. Choi and Y.-J. Kim, Predator-prey equations with constant harvesting and planting, Journal of Theoretical Biology 458 (2018), 47–57.

[6] J. Chung, Y.-J. Kim, O. Kwon, and C. Yoon, Biological advection and cross-diffusion with parameter regimes, AIMS Mathematics (2019) 4(6), 1721-1744.

[7] L. Desvillettes, Y.-J Kim, A. Trescases, and C. Yoon, A logarithmic chemotaxis model featuring global existence and aggregation. Nonlinear Anal. Real World Appl. 2019
[8] Desvillettes, L., Laurençot, P., Trescases, A., and Winkler, M. (2023). Weak solutions to triangular cross diffusion systems modeling chemotaxis with local sensing. Nonlinear Analysis, 226, 113153.
[9] T. Funaki, H. Izuhara, M. Mimura, and C. Urabe, A link between microscopic and macroscopic models of self-organized aggregation, Net. Het. Media. 7 (2012).
[10] K. Fujie and J. Jiang, Global existence for a kinetic model of pattern formation with density-suppressed motilities, Journal of Differential Equations, 269 (2020), 5338–5378.
[11] K. Fujie and T. Senba, Global existence and infinite time blow-up of classical solutions to chemotaxis systems of local sensing in higher dimensions, Nonlinear Analysis 222 (2022), 112987.
[12] T. Hillen and K.J. Painter, A user's guide to PDE models for chemotaxis, J. Math. Biol. 58 (2009), pp. 183–217.
[13] H.-Y. Jin, Y.-J. Kim, and Z.-A. Wang. "Boundedness, stabilization, and pattern formation driven by density-suppressed motility." SIAM Journal on Applied Mathematics 78 (2018), 1632-1657.
[14] E.F. Keller and L.A. Segel, Initiation of slime mold aggregation viewed as an instability, J. Theor. Biol. 26(1970), 399–415.
[15] E.F. Keller and L.A. Segel, Model for chemotaxis, J. Theor. Biol. 30 (1971), 225–234.
[16] Y.-J. Kim, H. Seo, and C. Yoon, Asymmetric dispersal and evolutional selection in two-patch system, Discrete Continuous Dynamical Systems 40 (2019), 3571–3593.
[17] C.-S. Lin, W.-M. Ni, and I. Takagi, Large amplitude stationary solutions to a chemotaxis system, Journal of Differential Equations, 72 (1988)
[18] H. Manzanarez, J.P. Mericq, P. Guenoun, J. Chikina, and D. Bouyer, Modeling phase inversion using Cahn-Hilliard equations - Influence of the mobility on the pattern formation dynamics, Chemical Engineering Science, 173 (2017), 411–427.
[19] W.M. Ni and I. Takagi,, On the shape of least-energy solutions to a semilinear neumann problem, Communications on pure and applied mathematics 44 (1991)
[20] W.-M. Ni and I. Takagi, Locating the peaks of least-energy solutions to a semilinear Neumann problem, Duke Math. J. 70 (1993)
[21] A.M.Turing,The Chemical Basis of Morphogenesis, Philosophical Transactions of the Royal Society of London. Series B, Biological Sciences 237 (1952), 37–72.
[22] Z.-A. Wang and X. Xu, Steady states and pattern formation of the density-suppressed motility model, IMA J. Appl. Math. 86, 577-603 (2021)
[23] M. Winkler, Can simultaneous density-determined enhancement of diffusion and corss-diffusion foster boundedness in Keller-Segel type systems involving signal-dependent motilities?, Nonlinearity, 33, 2020
[24] C. Yoon and Y.-J. Kim, Bacterial chemotaxis without gradient-sensing, J. Math. Biol. 70 (2015), 1359–1380.
[25] C. Yoon and Y.-J. Kim, Global existence with pattern formation in cell aggregation model, Acta. Appl. Math. 149 (2017) 101–123.

(Kyunghan Choi)
Department of Mathematical Sciences, KAIST, 291 Daehak-ro, Yuseong-gu, Daejeon, 34141, Korea
Email address: khchoi@kaist.ac.kr

(Yong-Jung Kim)
Department of Mathematical Sciences, KAIST, 291 Daehak-ro, Yuseong-gu, Daejeon, 34141, Korea
Email address: yongkim@kaist.edu